2023 IMEKO TC-4 International Conference on
Metrology for Archaeology and Cultural Heritage
Rome, Italy, October 19-21, 2023

An innovative heuristic strategy for the management of buried scenarios with strong discontinuities

Raffaele Persico[1], Gianfranco Morelli[2], Giuseppe Esposito[3], Ilaria Catapano[3]

[1] *Department of Engineering of the Environment and the Territory DIAM, University of Calabria Via P. Bucci, Cubo 45 A, 87036, Rende (CS), Italy, raffaele.persico@unical.it*
[2] *Geostudi Astier s.r.l., Via E. Fagno 31, 57123, Livorno, Italy, gf.morelli70@gmail.com*
[3] *Institute for Electromagnetic Sensing of the Environment IREA-CNR, Via Diocleziano, 328, 80124 Napoli NA, esposito.g@irea.cnr.it catapano.it@irea.cnr.it*

***Abstract* – This contribute proposes a heuristic strategy for processing GPR data referred to scenarios characterized by strong buried discontinuities, for which the common assumption of a homogeneous soil drives to errors in the imaging. This can be the case of layered media or the case of electrically large buried cavities. Here, the focus is on the buried cavities and a combined time-depth conversion strategy, which is able to account for the different propagation velocities in the cavity and in the surrounding soil, is proposed. Results referred to simulated data provide a preliminary assessment of the achievable imaging capabilities.**

I. INTRODUCTION

Detection and imaging of shallow cavities (up to a few meters) is an issue of interest in GPR prospecting. Cavities can be natural or anthropic, can have some cultural value (crypts, tombs) or some relevance in forensic investigations (hidden passages, bunkers of criminals), and can be potentially dangerous because of possible collapses [1-3]. The detection of shallow cavities usually is a plane task because customarily they show a strong dielectric contrast with the embedding medium. However, the correct imaging of a cavity is not straightforward, mainly (among other possible reasons) because the depth extension of the cavity appears significantly compressed with respect to other targets. This is due to the fast propagation velocity of the electromagnetic waves occurring into the cavity with respect to the surrounding soil. Consequently, if there are further targets beyond the cavities, the GPR data processing performed by means of the commonly adopted commercial software provides an image of the scenario affected by an incorrect representation of the relative depth levels. This drawback can be overcome by means of a combined time-depth conversion [4-5], as described in the following, accounting for the propagation velocity of the waves both in the (empty) cavity and in the surrounding soil. In order to apply a combined time-depth correction, both top and bottom of the cavity must be recognized in the radargram and it is needed to understand from it that the anomaly at hand is a cavity. This is deducible from several features as the strong reflection, the inversion of polarity of the echoes from the upper and lower bound of the target and possibly an X shaped picture due to the lateral (supposed vertical) walls of the cavity. Under these conditions, the combined time-depth conversion strategy allows a more correct image of the scenario under test.

II. COMBINED TIME-DEPTH CONVERSION

The schematic sketch of the combined time-depth

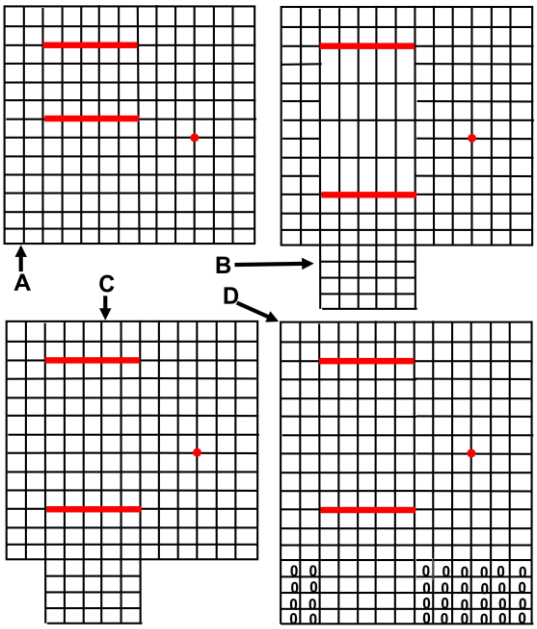

conversion strategy is shown in Fig. 1. Let us suppose that panel A represents (with abscissa and time along the horizontal and vertical axis) the result of a migration, performed making use of the propagation velocity of the medium surrounding the cavity. Customarily, the horizontal bounds of the cavity are well focused in this way, but the vertical size is not well represented because of the well-known compression effect due to the faster propagation velocity of the electromagnetic waves in the cavity.

However, if we identify that the target is a cavity (at least a probable cavity), then we know the propagation velocity of the waves inside it, and so we can re-expand the cavity at its real vertical size. In order to do this, we should convert the time-depth thickness of the cells by using the following vertical steps:

$$\begin{cases} \Delta z_s = \dfrac{c_s \Delta t}{2} \\ \Delta z_c = \dfrac{c_0 \Delta t}{2} = \dfrac{c_0}{c_s} \Delta z_s \end{cases} \quad (1)$$

In eq. (1), Δz_s represents the spatial vertical step of the retrieved image in the soil; c_s is the wave propagation velocity in the soil (retrieved e.g. from the diffraction hyperbolas); Δz_c denotes the spatial vertical step in the cavity and $c_0 = 30\ cm/ns$ is the wave propagation velocity in free space (because the cavity is supposed to be empty). Moreover, Δt is the time step of the data and the factor 2 at denominator is due to the round trip of the received signal. Equation (1) makes also evident that the ratio between the "natural" vertical sizes of the cells within the cavity and in the surrounding soil is equal to the ratio between the propagation velocity of the electromagnetic waves in free space and in the considered soil. This brings naturally to panel B in Fig. 1. Hence, the time-depth conversion should ideally account for the different wave propagation velocities in the soil and in the cavity. Consequently, we have an ideal result where some cells are vertically longer than the other ones within the image. Of course, the scheme of panel B is ideal and cannot be represented by means of a matrix, because it is implicit that the values of a matrix are attributed to cells having the same size. Therefore, a vertical interpolation of the cells within the cavity has to be performed.

On the basis of eq. (1), it is immediate to deduce that the number of cells within the cavity should be increased of an amount equal to the ratio between the wave propagation velocities in free space and in the soil, i.e., c_0/c_s. In general this ratio is not an integer number. So, after evaluating the theoretical output number of samples the closest integer has to be chosen. This introduces some distortion, but this imprecision it is of the order of one half of the vertical size of a cell, which in general is acceptable (if not, one could even increase the starting number of cells by means of a preventive vertical interpolation on the migrated result). This brings to the schematic result shown in panel C of Fig. 1 where, for simplicity of drawing, the vertical sizes of the cells have been represented according to an integer ratio equal to 2, which means to assume $c_0/c_s = 2$.

After the interpolation, however, we have the problem that the columns before and beyond the cavity have a smaller number of cells than in correspondence of the cavity. This is nothing strange from a physical point of view because a different average propagation velocity occurs along the columns of the resulting matrix. In other words, being the time bottom scale the same at any abscissa, the corresponding spatial depth will be not the same if we introduce the possibility of a different average propagation velocity vs the abscissa. Such a problem is easily solved by means of a zero padding, as depicted in panel D of Fig. 1. Let us note that in Fig. 1 the cavity is supposed to have flat top and bottom, which is not always the case. On the other hand, the extension to a more general curved ceiling and floor are immediate. It is, indeed, sufficient to calculate column by column the vertical interpolation of the cells within the cavity. This implies that a different number of samples is necessary for each column intercepting the cavity and consequently a different final zero padding occurs column by column. Finally, within the sketch of Fig. 1, we have also represented a point target. Such a point like target appears displaced below the cavity in the first image (panel A) in time domain, and it would "remain" below the cavity if a customary time depth conversion (performed according to the propagation velocity of the waves in the soil) were implemented. Instead, through the combined time-depth conversion strategy it is represented with its correct relative depth with respect to the cavity.

III. RESULTS

To state the imaging capabilities of the time-depth conversion strategy, we have simulated a Bscan by means of the open source code GPRMax (https://www.gprmax.com/, last consultation on May 22, 2023), which is based on the finite difference method in time domain and on the perfect matched layers with regard to the absorbing boundary conditions. The ground truth is represented in Fig. 2.

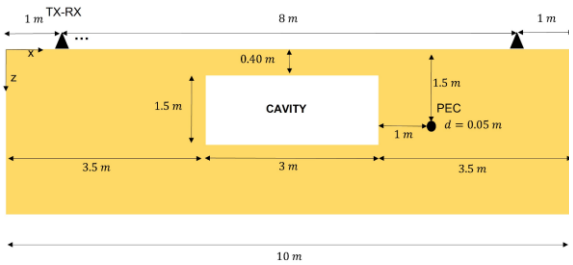

Fig. 2. Schematic of the simulated ground truth.

In particular, the Bscan is 8 m long, the spatial step of the data is 4 cm, the time bottom scale T is 80 ns and 4241 time samples are gathered at each measurement point. The source is a Ricker wavelet with central frequency at 400 MHz. The soil shows a relative dielectric permittivity equal to 9 and an electrical conductivity equal to 0.01 S/m. The cavity is large 3 m and extends from the depth to 0.4 m up to 1.9 m. Beyond the cavity, a metallic (perfect electric conductor) pipe is present too, at the abscissa 6.5 m along the Bscan and (referred to the centre) at the depth level of 1.5 m. The Reflexw commercial code (https://www.sandmeier-geo.de/reflexw.html, last consultation on May 22, 2023) performed the GPR data processing. Specifically, quite common procedures such as zero timing, background removal (limited to the first 5 ns) and gain vs depth were applied. In addition, radar traces were cleaned by means of a Butterworth filter in the range 150-850 MHz. Afterwards, the data were migrated in time domain according to a propagation velocity equal to 10 cm/ns, worked out from the diffraction hyperbola associated to the pipe, and exploiting 41 traces for the migration, based on the wideness of the diffraction hyperbola of the pipe. Before showing the reconstruction, a few radar traces gathered on the cavity are reproduced in Fig. 3, which shows a zoom of three traces picked up from the raw data, excluding in particular the initial strong reflection due to the air-soil interface. These traces show the echoes from the top and the bottom of the cavity, which shows an inverse polarity due to the passage from and optical denser medium to an optical less dense one (at the top) and then from an optically less dense medium to a denser one (at the bottom). This evidence together with the result achieved by processing the whole Bscan suggest (with high probability) that the encountered target is a cavity.

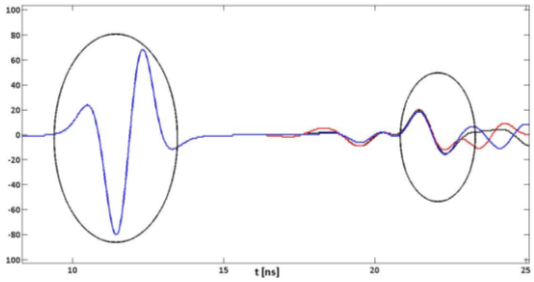

Fig. 3. Three radar traces on the cavity.

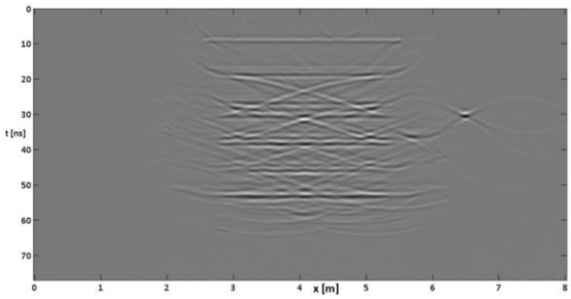

Fig. 4. Result of a migration algorithm.

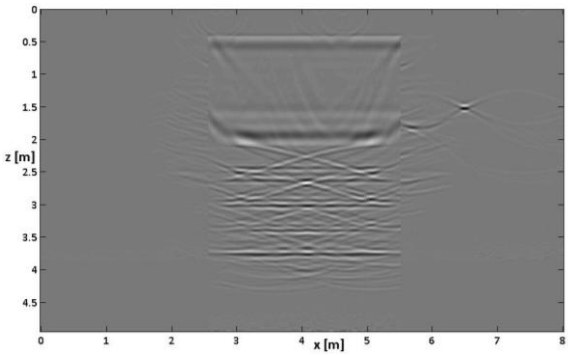

Fig. 5. Combined time-depth converted result.

Figure 4 shows the migration result represented in abscissa and time domain, while Fig. 5 shows the same result as converted in abscissa and depth by means of the proposed combined time-depth conversion strategy. As can be seen, the combined time-depth conversion provides a better image of the ground truth by reproducing the correct positional relationships between the point target and the cavity. Of course, a customary time-depth conversion based on the propagation velocity of the waves in the soil does not allow this, reproducing essentially the same image of Fig. 4, just re-scaled along the vertical axis.

IV. CONCLUSIONS

We have described a simple but effective way to perform the time-depth conversion in case of large cavities, which can occur in several GPR surveys and whose presence is often clued from GPR data. A result referred to simulated data has been provided, while experimental validations in controlled situations are ongoing. Furthermore, a future development is the simplification of the inputting of the up and down boundaries of the cavities by means of a computer graphic code. This code will speed the process especially when the upper and/or lower bound of the cavity are not flat and parallel to the air-soil interface. Another planned future development will be the execution of slicing directly in the spatial domain after combined time-depth conversion, thus having a three dimensional representation of the underground scenario closer to the ground truth.

REFERENCES

[1] F. Gabellone, G. Leucci, N. Masini, R. Persico, G. Quarta, F. Grasso, “Nondestructive Prospecting

and virtual reconstruction of the chapel of the Holy Spirit in Lecce, Italy", Near Surface Geophysics, vol. 11, n. 2, pp. 231-238, April 2013.

[2] G. Leucci, R. Persico, F. Grasso, L. De Giorgi, Integrated GPR Prospecting with the support of Historical Archive research and Historical Research: Three case studies in Lecce, Italy, International Journal on Conservation Science, vol. 6, n. 4, pp. 601-610, 2015.

[3] R. Persico, S. D'Amico, L. Matera, E. Colica, C. De, Giorgio, A. Alescio, C. Sammut and P. Galea, GPR Investigations at St John's Co‐Cathedral in Valletta. Near Surface Geophysics, vol. 17 n. 3, pp. 213-229. doi:10.1002/nsg.12046, 2019.

[4] R. Persico, F. Marasco, G. Morelli, G. Esposito, I. Catapano, A-posteriori insertion of information for focusing and time-depth conversion of Ground-penetrating radar data, Geophysical Prospecting, open access, https://doi.org/10.1111/1365-2478.13369, 2023.

[5] R. Persico, G. Morelli, Combined Migrations and Time-Depth Conversions in GPR Prospecting: Application to Reinforced Concrete, Remote Sens. 2020, Volume 12, Issue 17, 2778, open access, DOI 10.3390/rs12172778.